Journal of Biomedical Optics

SPIEDigitalLibrary.org/jbo

Real-time, *in vivo* measurement of tissular pO_2 through the delayed fluorescence of endogenous protoporphyrin IX during photodynamic therapy

Filippo Piffaretti
Anna Maria Novello
Rajendran Senthil Kumar
Eddy Forte
Cédric Paulou
Patrycja Nowak-Sliwinska
Hubert van den Bergh
Georges Wagnières

SPIE

Real-time, *in vivo* measurement of tissular pO_2 through the delayed fluorescence of endogenous protoporphyrin IX during photodynamic therapy

Filippo Piffaretti, Anna Maria Novello, Rajendran Senthil Kumar, Eddy Forte, Cédric Paulou, Patrycja Nowak-Sliwinska, Hubert van den Bergh, and Georges Wagnières
Medical Photonics Group, Swiss Federal Institute of Technology, SB-ISIC, Station 6, Lausanne, Switzerland

Abstract. Tissular oxygen concentration plays a key role during photodynamic therapy (PDT). Therefore, monitoring its local oxygen partial pressure (pO_2) may help predict and/or control the outcome of a PDT treatment. The first real-time, *in vivo* measurements of the pO_2 in the chicken egg's chorioallantoic membrane, using the delayed fluorescence of photoactivable porphyrins (PAPs), including protoporphyrin IX (PpIX), as monitored with a dedicated optical, fiber-based, time-resolved spectrometer, are reported here. The formation of PAPs/PpIX, photosensitizers of extensive clinical use, was induced in the chicken egg's chorioallantoic membrane (CAM) with aminolevulinic acid. An excellent correlation between the vascular damage induced by PDT and the reduction in tissular pO_2 is found. This study suggests that clinical measurement of the pO_2 using the PAPs'/PpIX's delayed fluorescence (DF) may be used to individualize in real time the PDT light dose applied. [DOI: 10.1117/1.JBO.17.11.115007]

Keywords: delayed fluorescence; oxygen partial pressure; protoporphyrin IX; photodynamic therapy; tumor.

Paper 12244 received Apr. 21, 2012; revised manuscript received Oct. 9, 2012; accepted for publication Oct. 10, 2012; published online Nov. 9, 2012.

1 Introduction

Due to its partial selectivity and minimally invasive character, photodynamic therapy (PDT) is often chosen for treating early stages of local, superficial cancers in hollow organs and other regions of the body accessible to light application.[1,2] PDT is also considered as the treatment of choice for, among others, actinic keratosis (in dermatology), and wet age-related macular degeneration (in ophthalmology). To obtain the desired cytotoxic and healing effects, PDT relies on the presence in the target tissue of a photosensitizer (PS), molecular oxygen (O_2), and administration of light at wavelengths absorbed by the PS. In this work, a time-tested method involving a biochemical precursor of the PS is used: topical or systemic administration of 5-aminolevulinic acid (ALA) leads, after a suitable drug-light interval, to biosynthesis and accumulation of photoactivable porphyrins (PAPs), including protoporphyrin IX (PpIX), the actual PS in the cells of the target tissue.[3] Note that ALA-derivative-based PDT procedures are now approved for the treatment of premalignant and malignant conditions in dermatology.[1]

Despite encouraging results, some clinicians avoid using this therapy due to observed fluctuations in intra- and inter-patient therapeutic outcomes.[4] These fluctuations, generally linked to uneven PS and/or O_2 tissular distribution, might in principle be counterbalanced by monitoring in real time the local PS and/or O_2 concentrations and then adjusting the light dosimetry.[5,6] Measuring the local pO_2 is also of interest for other types of treatments, such as radiotherapy, as it is well established that tissue oxygenation plays an important role in the outcome of such treatments.[7] Note that previous studies[8,9] have provided strong evidence that singlet oxygen ($^1O_2$) and other active oxygen species are the major active cytotoxic particles within the target tissues, which induce cell apoptosis. Therefore, accurate monitoring of $^1O_2$, though quite difficult to do, might lead to a better prediction of the clinical outcome than other monitoring techniques. However, optimizing the treatment dosimetry obviously remains a challenge.[10–13]

Different approaches have been proposed to monitor PDT efficiently, with the goal of improving its clinical outcome.[14,15] One of them is explicit dosimetry, in which the quantities of light, drugs, and oxygen are continuously and separately monitored during treatment. Alternatively, implicit dosimetry uses an indirect estimator of the biological damages, such as the degree of bleaching (photodegradation) of the photosensitizer, to predict the clinical outcome.[5,16,17]

This study uses the chicken embryo chorioallantoic membrane (CAM), an *in vivo* model well suited to characterize PDT's vascular effects,[18–20] to study the relationship between the evolution of tissular oxygen concentration during PDT and the resulting vascular damage. For this purpose, the quenching of PpIXs (from here on, the abbreviation PpIX encompasses both PpIX itself and the other photoactivable porphyrins) and delayed fluorescence (DF) by molecular oxygen[21] are measured on the one hand by a fiber-based spectrometer[22] to estimate pO_2, and on the other hand, on a simple, microphotographic-based evaluation index of the amount of vessel damage. The results of this study show that a robust, positive correlation exists between the reduction of tissular oxygen and PDT-created tissular damage.

Address all correspondence to: Georges Wagnières, Medical Photonics Group, Swiss Federal Institute of Technology, SB-ISIC, Station 6, Lausanne, Switzerland. Tel: +4121 693 3120; Fax: +4121 693 3626; E-mail: georges.wagnieres@epfl.ch

0091-3286/2012/$25.00 © 2012 SPIE

2 Materials and Methods

2.1 *PpIX Photodynamics and Diffusional Properties When Used as the PS*

A summary of the photochemically induced reactions (type-II photochemical reaction pathway) can be represented by the following chemical scheme:

$S_0 + h\nu \rightarrow S_1$	Photon absorption by the PS
$S_1 \rightarrow T_1$	Intersystem crossing
$T_1 + {}^3O_2 \rightarrow S_0 + {}^1O_2$	Collisional energy transfer between PS and molecular O_2

S_0 is the singlet ground state of the PS, which is excited (upon absorption of a photon of energy $h\nu$) to the first excited singlet state S_1. The latter can undergo intersystem crossing with a certain quantum yield (approx. 60% for PpIX, measured in *in vitro* conditions)[23] to the long-lived triplet state T_1, which has a lifetime ranging from a few microseconds up to a few milliseconds. This is why the tissular oxygen in the triplet ground state ($^3O_2$) has enough time to undergo a collision with the PS in the T_1 state, to form the highly reactive and cytotoxic singlet molecular oxygen $^1O_2$. Once generated, $^1O_2$ undergoes deexcitation through several pathways, among which a low-probability radiative decay with emission of an infrared photon at 1270 nm. This $^1O_2$ luminescence is in fact characterized by a very weak signal, making its measurement not easily applicable in the clinical context (the luminescence emission of $^1O_2$ has a probability of 10^{-8} and a characteristic lifetime of approx. 100 ns under *in vivo* conditions).[10,24] These fast and weak signals from $^1O_2$ at 1270 nm are difficult to work with, especially under clinical conditions.

The idea was developed to measure the production of excited singlet oxygen via the "consumption" of the PpIX's triplet state (T_1 in the above chemical scheme), which is efficiently quenched by the molecular oxygen found in the tissue. Indeed, a fraction ranging from 55% to 80% of the PpIX T_1 population is quenched by $^3O_2$, depending on the actual conditions.[23] Therefore, measuring the photosensitizer's luminescence lifetime offers an alternative to measuring the radiative decay of $^1O_2$.[25] Furthermore, in contrast to intensity measurement methods, lifetime measurement methods have the advantage of being inherently self-referential and more robust.[26]

PpIX's phosphorescence signal, from the radiative path connecting T_1 to S_0, may not be detected easily *in vivo* because the phosphorescence quantum yield is much too low and because this luminescence takes place at wavelengths too long to be easily detected.[27] This difficulty can be overcome by measuring PpIX's DF lifetime as a substitute for its phosphorescence lifetime.

2.2 *Principles and Experimental Setup for pO_2 Determination Through the Measurement of the PS's DF Lifetime*

Tissular pO_2 can be determined by measuring the lifetime τ of the PS's triplet state, thanks to the Stern-Volmer relationship:

$$I_0/I = \tau_0/\tau = 1 + K_q \cdot pO_2, \quad (1)$$

where I and τ refer to the intensity and lifetime of the PS's phosphorescence for a given tissue pO_2, while I_o and τ_o refer to the values measured in the absence of oxygen and K_q is the Stern-Volmer constant. In this study, tissular oxygen concentrations are given as values of pO_2 in units of percent (%), meaning that the tissue is assumed to be saturated and in equilibrium with an oxygen-containing gaseous mixture (usually air or calibrated nitrogen/oxygen mixtures) at a pressure of 1 atm. The lifetime τ is determined indirectly, by detecting the DF of the PS's excited triplet state. For this purpose, a fiber-based, time-resolved spectrofluorometer was used. It is described in details in Ref. 28, including the setup's temporal resolution and level of background optical noise. The schematics of the experimental setup are shown in Fig. 1.

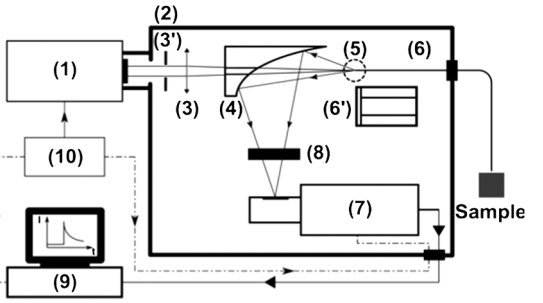

Fig. 1 Schematic of DF experimental setup. Its components are (1) pulsed (≈0.5 ns) dye laser; (2) experimental enclosure with a 3′ diaphragm; (3) lens, (4) parabolic mirror with cylindrical hole; (5) focusing location; (6) optical fiber; (6) thermostabilized cell holder; (7) gateable photomultiplier; (8) optical filters holder; (9) digital storage oscilloscope and PC; and (10) pulse and delay generator.

The plano-convex lens (3) is mounted on a 5-degrees-of-freedom holder, allowing for easy focusing of the laser beam on a predefined point (5) (for specific details about the setup or parts thereof, see Ref. 28). The luminescence emitted from the irradiated sample is collected by the distal end of the optical fiber (6) and returned to the enclosure, where a large fraction (probably more than 80%) of this light falls on the parabolic metal mirror (4) and is reflected and focused by it on a gateable photomultiplier (PMT) (7). The reflected laser light and unwanted optical background noise are filtered out by a band-pass filter in the filter wheel (8; center wavelength: 645 nm, full width at half maximum: 75 nm). The PpIX DF signal is recorded with a digital storage oscilloscope (DSO) connected to a PC (9), where the data processing and analysis takes place (see the next section for more detail). The signal delay generator (10) is used to synchronize the gating of the PMT with the laser pulses and to trigger the DSO with the DF signals. The advantages of this optical design include (a) the absence of spectral distortions because only reflections take place in the scrutinized part of the optical path; (b) no autoluminescence is induced in the parabolic mirror which, due to its metallic nature, does not interact with the excitation pulse; (c) the solid angle of acceptance of the parabolic mirror (≈0.6 sr) is larger than the entrance solid angle of the optical fiber (≈0.15 sr), which leads to a high light recovery fraction; (d) the mirror's parabolic shape eliminates the need of an additional lens to focus the luminescence emitted by the fiber tip (or the quartz cuvette) on the detector.

The time-resolved detection of the weak DF signal requires gating to avoid saturation of the detector by the much stronger prompt fluorescence (PF) signal. The photomultiplier tube is switched on about 3 μs after the laser pulse, allowing the intensity of any PF to decrease to the noise level.

2.3 *Data Acquisition and Analysis*

The PMT's analog signal is supplied to the DSO for averaging (about 30 transients are used), and the averaged values are transferred to the PC for analysis. The luminescence decay is fitted to a sum (usually one or two components are retained) of exponential functions:

$$f(t) = \sum_{i=1}^{n} A_i \exp^{(t/\tau_i)}. \quad (2)$$

The Levenberg-Marquardt method was chosen for these nonlinear least-squares fits,[25,29–31] using a self-written algorithm implementation. The calculated mathematical fits were graphically checked by plotting the residuals of each fit and the autocorrelation of the residuals,[32,33] as shown in previous research.[28]

2.4 *Handling of the CAMs and ALA Administration*

The procurement and processing of the eggs to prepare the CAM has been described in previous research (such as Ref. 20). In brief, fertilized chicken eggs are transferred (blunt end up) into an automatic turn-incubator, set at 37°C, 65% relative humidity (RH), and normal atmospheric pO_2 conditions (i.e., 21%). Given the geographical location (400 m above sea level) of the experimental setup, this corresponds to a partial pressure of approximately 150 mmHg of O_2. On embryo development day 3 (EDD 3), a portion of the eggshell is removed at the pointed end of the egg, creating a hole of approximately 3 mm in diameter, which is covered with Parafilm cling film, and the pointed end is always kept pointing up. This procedure causes the embryo and its enveloping CAM to retract locally from this artificial opening, exposing at its surface a flattened portion of the membrane, and providing an access to observe and treat the CAM's capillary plexus and vasculature. The eggs are then returned to the incubator (blunt end down) and kept in a static position. At EDD 11, the eggs are removed from the incubator for topical ALA administration: a zone of the CAM characterized by homogeneous vascularization is visually selected and a 20 μl droplet of a 0.15 M (20 mg/ml) ALA aqueous solution in 0.9% NaCl, adjusted to pH 6 with NaOH, is deposited in the center of this zone. The eggs are then returned to the incubator and kept static until further use. As a rule, any manipulation of the CAM after ALA application is performed in total darkness or under subdued light.

2.5 *PpIX Buildup Kinetics After ALA Topical Administration*

Limited experimental data have been published about the localization and buildup kinetics of PpIX in the CAM following topical administration of ALA. Moreover, most of the results have been obtained for tumors growing in this membrane.[34–36] In view of optimizing DF signal quality, a first experiment using 10 eggs is performed, whereby each egg is examined during times ranging between 0 to 6 h following the topical administration of ALA.

In Fig. 2(a), the resulting spatial distribution of PpIX in the CAM is shown, 4 h after ALA administration. The picture reveals a slightly more intense fluorescence (lighter areas) near the walls of the large vessels. As an illustrative example, the luminescence intensity in the administration zone is presented in Fig. 2(b). As shown in this figure and in agreement with Refs. 34–36 the maximum of PpIX accumulation is reached approximately 4 h after ALA administration.

2.6 *PDT Irradiation and CAM Tissular Oxygen Depletion Measurements*

The study design is guided by the following rationale (see below for description of experimental protocols): Protocol I is used to determine the existence of a robust relationship between PDT duration (up to 600 s) and pO_2, while using a minimum number of eggs: thus, each egg is submitted to a number of successive, cumulative irradiations and measurements.

Protocol II seeks to check the same relationship as protocol I using (a) a different batch of eggs, (b) intermediate durations for the incremental PDTs, and (c) a longer total treatment time (900 s), in order to confirm and improve the precision of the relation observed using protocol I, while still keeping the cumulated total measurement time under a certain maximum (6 times 3 s). In fact, in protocols I and II, pO_2 measurements are performed once during each 3 s OFF period of the treatment laser (i.e., immediately after each incremental PDT irradiation period) and the difference with the initially determined baseline pO_2 value is computed to be the tissular oxygen depletion assignable to the corresponding, cumulated, PDT treatment time.

Protocol III is used to prove that the parasitic effects of the multiple, intermediary, measurements used in protocols I and II are negligible (Fig. 3).

The normal, baseline value of the pO_2 is determined for each egg before any PDT irradiation protocol is started. The treatment

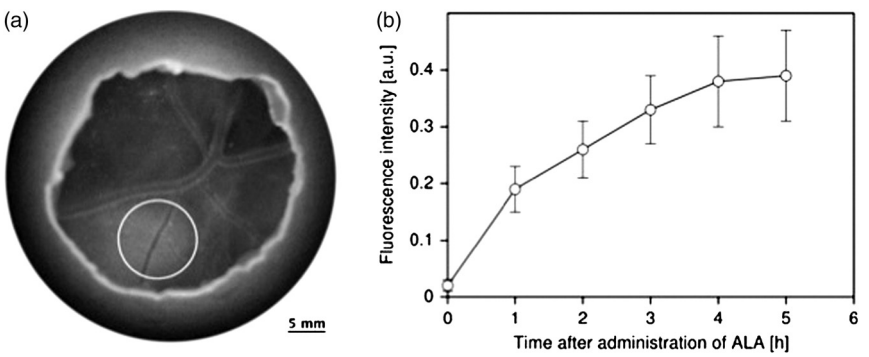

Fig. 2 Typical fluorescence image of a CAM, and plot of fluorescence pharmacokinetics measured on it. (a) PpIX fluorescence in the CAM model recorded 4 h after topical (white circle) administration of a droplet (20 μl) of 0.15 M ALA solution (λ_{ex} = 405 nm, λ_{em} > 460 nm); the heterogeneity of the PpIX fluorescence is clearly visible. (b) Fluorescence pharmacokinetics of the PpIX biosynthesis. Error bars represent the standard deviation.

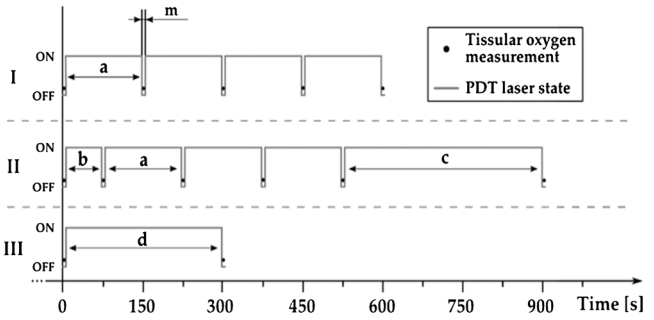

Fig. 3 Chronograms of the illumination and measurement protocols. Shown here are the cumulative PDT irradiations, interspersed with O_2 measurements during which the PDT source is suppressed. PDT irradiation times were: $a = 150$ s, $b = 75$ s, $c = 375$ s, $d = 150$–900 s, while the O_2 measurement duration was $m = 3$ s.

laser is then switched on and off and pO_2 measurements performed according to one of the three experimental protocols described above. In protocol III, pO_2 measurements are performed just once before and once after a continuous, predetermined irradiation period. The difference between those two pO_2 values is computed to be the tissular oxygen depletion assignable to the corresponding, uninterrupted, PDT treatment time.

Details of the PDT irradiation and tissular oxygen measurement procedures are as follows: At EDD 11, 4 h after ALA administration, the egg is taken out of the incubator and placed under the combined PDT-irradiation/DF-measurement setup. The drug-light interval of 4 h allows time for the cells to produce sufficient tissular PpIX. In order to minimize re-oxygenation of the tissue during PDT by atmospheric oxygen, a round, 20-mm, 0.15-mm-thick microscope cover-glass (3) is gently floated on the CAM's surface (1) after depositing two drops (2) of human physiologic serum (≈80 μl of 0.9% NaCl; see Fig. 4). This liquid layer, acting as a cushion, is essential to avoid any adherence between the cover-glass and the CAM and possible subsequent injury to the CAM surface. Therefore, during PDT or tissular oxygen measurement, oxygen may diffuse only from the CAM vasculature and from the tissues adjacent to the treated zone, not from the shielded surface of the treated zone.

A PDT treatment zone, featuring blood vessels and capillaries with diameters ranging from 5 to 300 μm, is visually chosen, approximately in the middle of the zone under the cover-glass. The tip of the optical fiber (5) is aimed toward the center of this zone and held at a distance of ≈100 μm above the cover-glass. It is kept in place by a metal fiber holder (6). The PDT light is provided by a CW solid-state diode laser (2) (Oxxius, 405 nm, 1.3 mW total power at the distal end of the fiber) and administered through a light distributor providing a homogenous spot (4) (MedLight Frontal light distributor, NA = 0.37, core diameter 600 μm). This treatment fiber was chosen and its distance to the CAM adjusted so as to deliver a homogeneous PDT treatment spot (diameter 8 mm) on the selected zone of the CAM vasculature. Small irradiances (≈2.5 mW/cm^2) are preferred to avoid significant photothermal effects. The period during which the eggs are kept out of the incubator is limited to about 15 min. To keep the DF measurement durations small with respect to PDT exposure times, only 30 consecutive laser sweeps on the same area are used and averaged for the oxygen measurements. Thus, the total acquisition time for one measurement is 3 s, compared to a minimum PDT exposure time of 75 s, and the corresponding total light dose delivered by the probing laser is limited to ≈100 mJ/cm^2, as compared to a minimum PDT light dose of ≈190 mJ/cm^2, both at 405 nm. A light dose of 100 mJ/cm^2 is found to have a barely detectable PDT vascular effect. Therefore, the minimal PDT light dose is set to approximately double this value. At the end of the PDT treatment, the cover-glass is carefully removed from the treated zone. Only very small iatrogenic damages are identified after these mechanical operations. The eggs then are returned to the incubator while waiting for the vascular damage assessment.

2.7 *Vascular Damage Assessment*

The treated eggs are taken out of the incubator 16 to 18 h after termination of the PDT irradiation protocol. This standard time period has been in use in our laboratory for several years, partly for practical reasons, as the measurements are performed overnight.[37] Although it was not methodically optimized, it corresponds to a state of the CAM where PDT damage has had the time to develop further while the counteracting processes of vessel repair and neo-angiogenesis have not yet interfered significantly with the PDT results.[37]

An intravenous (IV) injection of 20 μl of a 150 μM solution of fluorescein isothiocyanate-dextran (FITC-dextran, 150 kDa, 25 mg/ml in NaCl 0.9%, Sigma Aldrich) is administered into one of the large CAM veins, while 0.1 ml of India ink (Parker-Quink) is injected under the CAM into the extraembryonic cavity to increase contrast and screen out the continuously changing background fluorescence.[38] Vascular damage due to PDT is then examined and recorded photographically with an epifluorescence microscope (Nikon E600FN, excitation wavelength between 450 and 490 nm, emission wavelength >520 nm). The damage extent is classified on the basis of blood vessel closure: The diameter of the largest blood vessels closed by the PDT

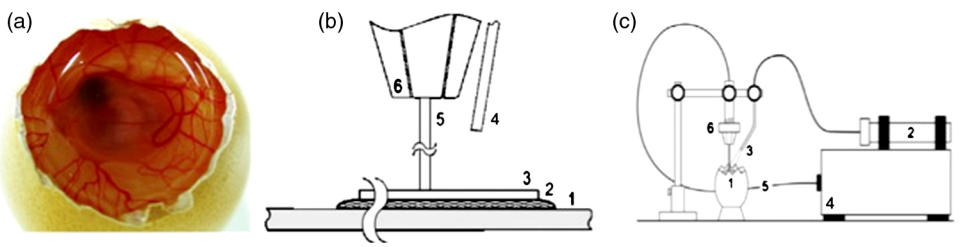

Fig. 4 Description of the CAM study experimental apparatus. (a) Top view of a CAM membrane ready for an experiment. (b) Details of a tissular oxygen measurement: (1) CAM membrane; (2) protective drop of aqueous serum; (3) 0.19-mm cover-glass; (4) PDT treatment fiber; (5) excitation/probing fiber; (6) fiber holder. (c) (1) CAM in the open egg; (2) PDT treatment laser; (3) fiber used for PDT irradiation; (4) time-resolved spectrofluorometer with dye laser excitation source; (5) excitation and probing fiber; and (6) fiber holder.

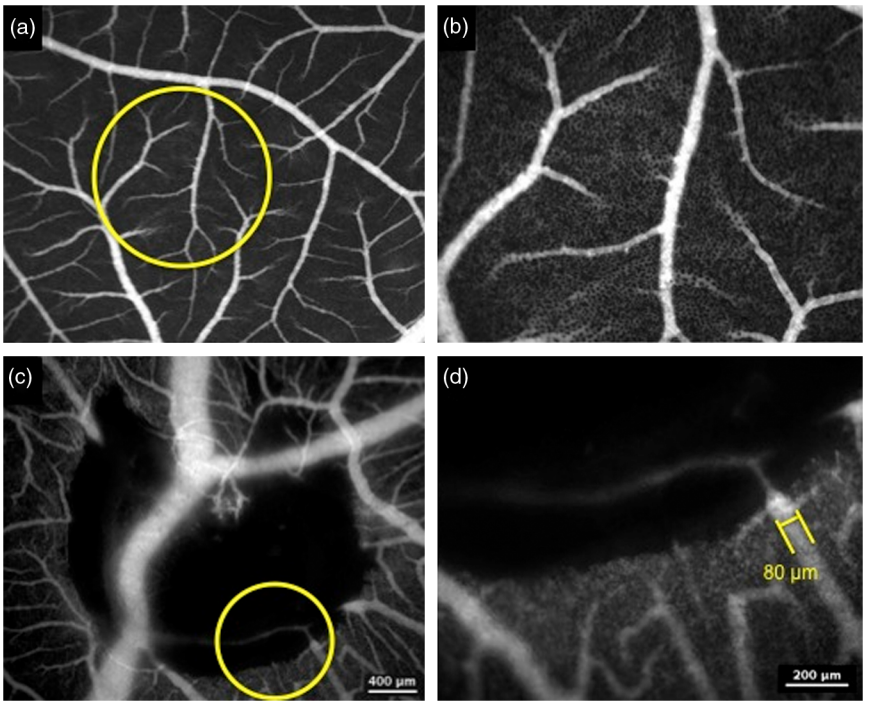

Fig. 5 Fluorescence images of CAM vessels at various magnification factors. PDT-induced vessel damages in the CAM model made visible by an IV injection of FITC-dextran, drug-light interval of 4 h. (a) and (b) before any PDT irradiation, intact vessels; (c) and (d) vascular damage observed 17 h after irradiation with 2.25 J/cm^2 at 405 nm, 2.5 mW/cm^2, laser spot diameter: 5 mm. (a) and (c): objective 4×; (b, d) objective 10×.

treatment is used as an arbitrary index of vascular damage. Figure 5 shows examples of actual micrographs.

A drug-light interval of 4 h was chosen for the PDT procedure and used throughout this study [see Fig. 3(a) and 3(b) for the experimental determination of this time interval]. The zone where ALA is topically administered then is selected to perform DF measurements, as this results in an adequate signal-to-noise ratio. The treatment laser delivers 2.5 mW/cm^2 at 405 nm.

3 Results

3.1 *In Vivo Measurement of Tissular* pO_2 *as a Function of PDT Irradiation Time*

In a first series of experiments, DF-based O_2 measurements were performed on a number of egg batches (each one comprising 12 to 20 eggs), subjected to increasing cumulated PDT irradiation times. Three slightly different illumination protocols were used (see Fig. 4 and PMGQ3PMGQ and Sec. 2 of this paper).

The left vertical scale of Fig. 6 shows the measured reciprocal lifetime of PpIX's DF plotted against the total illumination time (horizontal axis). The right vertical scale of the figure gives the corresponding (computed) tissular pO_2, using the Stern-Volmer equation, in which K_q was derived from previous experiments.[22]

Clearly, the tissular oxygen concentration decreases during the first 500 s of cumulated PDT time, for a cumulated light dose of 1.25 J/cm^2. At longer treatment times, it reaches an asymptotic residual value, close to zero. The relatively large error bars (±1 standard deviation) probably relate to inhomogeneities in the distribution of the PS and/or local differences in the aptitude of CAM tissues to renew the O_2 consumed by the PDT process, depending on their level of metabolism and

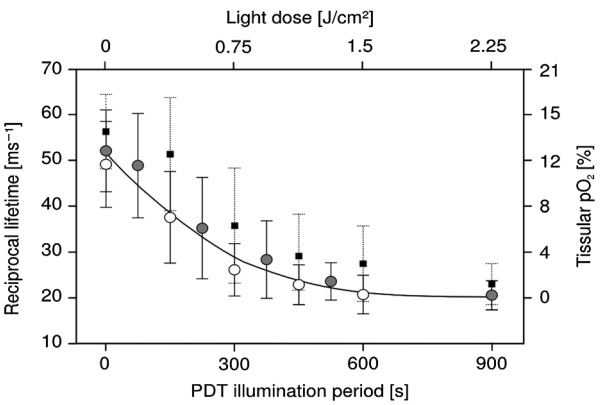

Fig. 6 Plot of DF and oxygen partial pressure in tissue during PDT treatment. DF reciprocal lifetime of PpIX in the *in vivo* CAM model as a function of PDT duration. Protocol I (○), Protocol II (•), Protocol III (■). The curve is presented for visual assistance only.

degree of vascularization. It can be seen that differences ascribable to illumination protocol, if any, are negligible in this experimental context.

3.2 *Tissular Oxygen Depletion as an Index of PDT Efficiency*

A second experiment was then performed on five lots of 20 eggs, submitted to different PDT optical doses, using illumination Protocol III (see above for details of egg/CAM handling).

The baseline value of tissular pO_2 was first determined for each untreated egg before starting the chosen PDT irradiation protocol, using the described PpIX DF reciprocal lifetime determination. The eggs were then submitted to PDT illumination

under a constant irradiance of 2.5 mW/cm^2 at 405 nm for different durations (150, 300, 450, 600, 900 s), corresponding to optical light doses of 0.38, 0.75, 1.14, 1.50, and 2.25 J/cm^2, respectively.

Immediately after treatment, each egg's tissular O_2 concentration was again measured with the same method. The difference between the initial and final DF reciprocal lifetimes was used as a measure of tissular O_2 depletion ascribable to the PDT treatment. Figure 7 illustrates this increasing oxygen depletion as a function of PDT illumination time.

The eggs were then returned to the incubator for 16 to 18 h. Finally, the extent of vascular damage caused by the PDT was determined using a simple arbitrary damage index described above.

In Fig. 8(a), the vascular damage index is plotted as a function of the PDT treatment duration. As expected, the data shows a clear, positive correlation between those two parameters. Although, as already noted, the tissular pO_2 does not decrease significantly anymore for PDT illumination periods longer than about 500 s (Fig. 6), the observed tissular damage does continue to increase with increasing light doses, at least until the irradiation time of 900 s. This suggests that the PDT mechanism is still operating at very low oxygen concentrations.

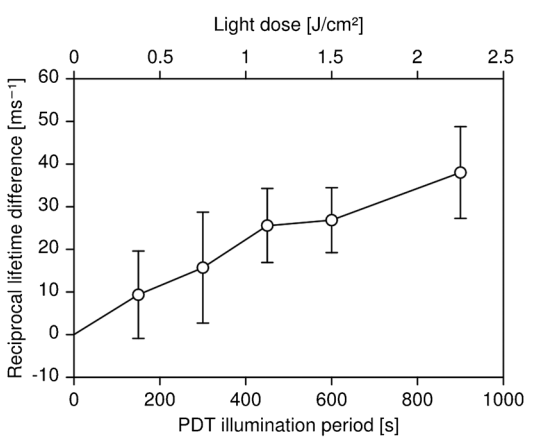

Fig. 7 Reciprocal lifetime difference as a function of PDT illumination time. Error bars represent standard deviations. The curve is presented for visual assistance.

Figure 8(b) shows the vascular damage index as a function of the reciprocal lifetime difference, a measure of tissular oxygen reduction during the treatment. Here again, a strong, positive correlation between the two parameters is clearly visible.

4 Discussion

This paper reports a first study aiming at measuring, *in vivo* and in real time, the level of molecular oxygen contained in tissue, using the DF of a PS, in order to optimize PDT. The results demonstrate a clear correlation between the PDT-induced vascular damage and the reduction in tissular oxygen concentration, as assessed by the change in DF lifetime. This agrees with previous works[8,9,39,40] regarding the role played by oxygen in PDT-induced tissue damage. Thus, adjusting the PDT light dose based on a real-time estimate of tissular pO_2 monitored through the PS's DF appears feasible. This approach then might enable controlling the efficacy of PDT, and reducing intra- and inter-patient fluctuations in this treatment's clinical outcome.

The method presented here does not require the use of exogenous oxygen sensors since it is based on detecting the DF of the PS itself. This feature is important because, besides ALA, several other precursors of PpIX are now approved by the medical authorities of a number of countries. This is an implicit light dosimetry method because the pO_2 value (or its reduction, both being related to the production of singlet oxygen) is measured close to the PS (about 1 μm). Such a method is likely to be much more directly related to PDT's tissular effects than approaches relying on explicit light dosimetry (light dose, PS global concentration, etc.).[5,16,41–43] In addition, most of these other methods for quantifying the outcome of PDT suffer from the fact that the pO_2 is not measured at a subcellular or tissular scale.

In similar research, Mik et al. report *in vitro* and *in vivo* experiments using PpIX's DF lifetime signals, to assess the amount of oxygen in tissues.[27,44] However, as compared to other oxygen-sensing techniques, DF measurements have the advantage that they record the oxygen concentration in close proximity to the photosensitizer. In fact, given the diffusivity of molecular oxygen ($^3O_2$) in tissue ($D \approx 1.7 \cdot 10^{-5}$ cm^2/s),[45,46] and using PpIX's triplet state maximum lifetime *in vivo* ($\tau \approx 60$ μs), the distance reachable by an O_2 molecule to interact with excited PpIX molecules is calculated to be on the order of ≈ 1 μm ($\delta = \sqrt{(6D_\tau)}$).[47] If the same computation is done for singlet oxygen ($^1O_2$), characterized by much shorter lifetime

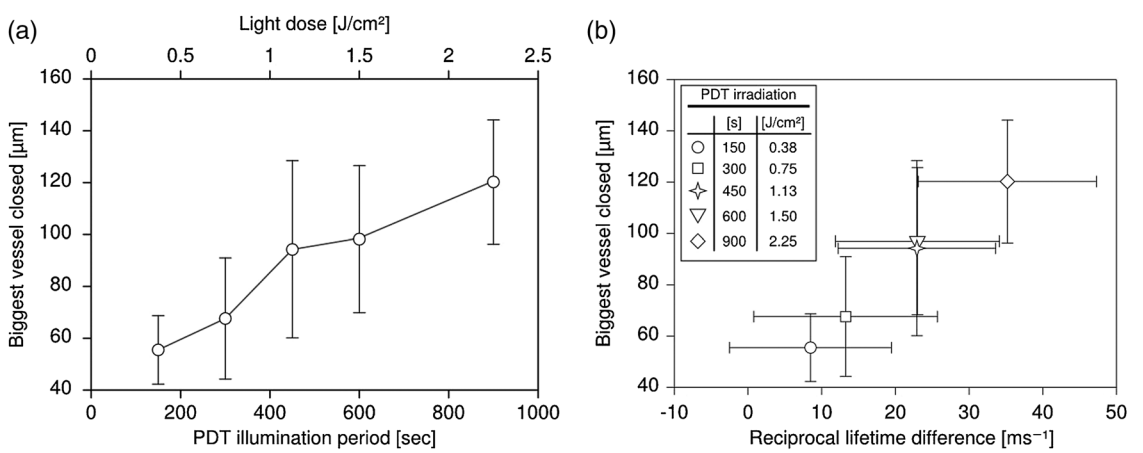

Fig. 8 Plot of PDT-induced vessel damages in the CAM model. (a) As a function of PDT duration; (b) as a function of tissular oxygen reduction, taken as the difference between final and initial reciprocal PpIX DF lifetimes. Error bars are standard deviations.

of approximately 250 ns, the reachable radius is less than 40 nm,[24] indicating that the photo-damages are induced at the close vicinity of the photosensitizing molecule. On the other hand, the critical oxygen diffusion distance, usually defined as the distance between a hypoxic tissue (i.e., a tissue in a situation of critically low oxygen level) and the nearest vessel was measured by Grote et al. to be on the order of 100 μm in a tumoral tissue.[45] It is therefore clear that this DF-based oxygen sensing method is able to spatially discriminate between hypoxic zones and normally oxygenated tissue, providing that the excitation and/or emission light are administered and/or detected with the appropriate resolution. It is also worth noting that during the several hours of incubation, ALA is absorbed by the vasculature, where it circulates, and then diffuses out of the vasculature into almost all egg tissues. This is why PpIX are formed and accumulated apparently with different concentrations in most of the tissues of the chicken embryo.

Since in this study both the light used to excite the DF and the light used for PDT have the same wavelength, the DF excitation might itself induce some level of pO_2 reduction, PpIX photobleaching, and vascular damage, thus leading to artifacts. However, the DF excitation light dose used here is much smaller than the one used to induce the smallest detectable PDT effect, and in a previous study,[22] it was demonstrated that, in the absence of PDT irradiation, the DF excitation light does not induce any detectable vascular effect in similar conditions. Finally, the DF lifetimes measured with the three different illumination protocols confirm that the contribution to vessel closure of this excitation light (which differs according to the protocol used) is negligible (see Fig. 6).

A drug-light interval of 4 h was used for the present study. It should be noted that other incubation periods may lead to other values of the DF lifetimes, even if all other conditions are identical, since it is well known that the PpIX buildup, which takes place in specific tissue/cellular compartments, is followed by a diffusion of the PS to other compartments that present other microenvironments.[48] The changed microenvironments then may lead to changed local pO_2 and hence change in DF lifetime, as well as changed vascular occlusion efficiency. As a consequence, it could be that the results reported in Figs. 6 and 8 may differ if longer or shorter drug-light intervals are used.

The relatively large error bars affecting the DF lifetimes presented in Figs. 6–8 may well be due to local differences in tissue oxygen renewal during PDT. These local differences could, for example, be due to spatial and/or temporal differences in the metabolic activity, blood perfusion, inhomogeneous distribution of the PS, etc. Therefore, one approach to reducing these fluctuations would consist of probing a larger area (typically 1–2 cm in diameter) so that the measurement is averaged over a larger surface. These observations furthermore suggest that it might be of interest to image the PS's DF lifetime at "high" spatial resolution in the hope of getting information regarding the changes of tissue oxygenation at a tissular and even a cellular level. Recording such images at different times after the beginning of PDT and at different drug-light intervals would certainly help to identify treatment strategies to target specific tissue structures (vessels versus stroma, for instance).

Finally, it should be noted that due to the instrumentation and the shot noise, the fluctuations affecting the DF lifetime measurements are negligible compared to the other factors mentioned above. Indeed, repeated measurements performed in identical conditions, at the same location and on the same sample, confirm this. Nevertheless, if necessary, the shot noise can be improved further by reducing the time during which the detector is blinded to reject the prompt fluorescence. The resulting increase of DF radiant energy detected will decrease the shot noise, but it also will increase the risk of detecting (a) the emission of other endogenous luminophores presenting "long" (i.e., between 100 ns and 1 μs) luminescence lifetimes; and (b) luminescence emitted by the instrumentation (laser spontaneous emission, luminescence from the optics in the setup). This is why, in this study, a time delay of 3 μs was selected to "blind" the detector, which corresponds to an optimal tradeoff between this delay and the observed signal-to-noise ratio.

The error bars affecting the measurements of the diameter of the largest occluded blood vessels, which are shown in Fig. 8 are likely to be due to various factors, including the following:

(a) The selection of the area treated by PDT. Indeed, somewhat different results may be obtained if the relative density of large and small vessels, or of veins versus arteries, differs from place to place. Although the relative importance of this source of fluctuations is difficult to assess quantitatively, it probably plays a minor role, as described by Lange et al.[20] who used a similar metric to quantify the vascular effects induced by PDT in the CAM model.

(b) The inhomogeneous distribution of PpIX, as reported by many studies.[49,50]

(c) Intrinsic errors while measuring the vessels diameter. The fluctuations due to this last element could be reduced using quantitative image analysis programs to characterize the vascular network, as proposed by Ref. 51. One may conclude, considering the above-mentioned factors, which are possibly responsible for the rather large fluctuations affecting measurements of the DF lifetime and blood vessel closure efficacy, that probing of larger well-selected areas, as indicated above, most likely will help to reduce these fluctuations.

The results presented in Fig. 8(b) indicate that the vascular occlusion effects of PDT and the differences in reciprocal DF lifetime, which is a metric for the tissular oxygen reduction, are correlated. For illumination periods longer than 500 s (1.25 J/cm^2), it is noteworthy that the vascular damage continues to increase, despite the fact that the measured residual pO_2 does not decrease significantly anymore after 500 s (it is then already very close to 0%, as shown in Fig. 6). This indicates that some PDT-related mechanism continues to be effective at very low pO_2. One possible explanation is that all the oxygen provided by the bloodstream is consumed immediately during the PDT illumination. This hypothesis is realistic since the blood vessels affected by PDT, depending on their size among others, will close to a large extent, after the end of the illumination,[52] at the applied conditions. Consequently, in such conditions, the PDT effect would be "oxygen supply dependent," as reported elsewhere.[53–55] Other phototoxic mechanisms that do not involve molecular oxygen, as suggested by Plaetzer et al.,[56] could also cause a PDT effect in the absence of a significant pO_2. It is possible that experiments similar to those presented in this paper, but performed at different fluence rates, may help to reveal the nature of these effects.

Finally, note that the approach presented here is of interest, not only for PpIX-based PDT, but also when other PSs with a

detectable DF or a difficult-to-detect phosphorescence is used. One may even suggest that the technique presented in this paper be used to monitor the pO_2 during the treatment of age-related macular degeneration (AMD) with Visudyne®. Indeed, application of the DF measurements to the retina may be helped by the unique optical properties of the eye, and using such measurements may help compensate, to some extent, for the inter-patient fluctuations observed during AMD-PDT.[57]

In conclusion, the present work has demonstrated *in vivo* that the DF of a photosensitizer can be used to determine the pO_2 in tissues and help to predict PDT's tissular effects. Applications of this approach to other systems are numerous, and this technology may help improve understanding of the mechanisms involved in the oxygenation and photosensitization of various materials, including biological tissues.

Acknowledgments

This work was supported by the Swiss National Science Foundation (Grant No. 205320-130518) and funded in part by the J. Jacobi Trust. We gratefully acknowledge editorial support by Matthieu Zellweger.

References

1. P. Agostinis et al., "Photodynamic therapy of cancer: an update," *CA Cancer J. Clin.* **61**(4), 250–281 (2011).
2. A. Weiss et al., "Angiogenesis inhibition for the improvement of photodynamic therapy: the revival of a promising idea," *BBA Rev. Cancer* **1826**(1), 53–70 (2012).
3. N. Fotinos et al., "5-Aminolevulinic acid derivatives in photomedicine: characteristics, application and perspectives," *Photochem. Photobiol.* **82**(4), 994–1015 (2006).
4. S. Radakovic-Fijan et al., "Efficacy of three different light doses in the treatment of actinic keratosis with 5-aminolevulinic acid photodynamic therapy: a randomized, observer-blinded, intrapatient, comparison study," *J. Am. Acad. Dermatol.* **53**(5), 823–827 (2005).
5. T. Glanzmann et al., "Pharmacokinetics of tetra(m-hydroxyphenyl) chlorin in human plasma and individualized light dosimetry in photodynamic therapy," *Photochem. Photobiol.* **67**(5), 596–602 (1998).
6. T. M. Busch, "Local physiological changes during photodynamic therapy," *Lasers Surg. Med.* **38**(5), 494–499 (2006).
7. M. Arabi and M. Piert, "Hypoxia PET/CT imaging: implications for radiation oncology," *Q. J. Nucl. Med. Mol. Imaging* **54**(5), 500–509 (2010).
8. J. Moan and P. Juzenas, "Singlet oxygen in photosensitization," *J. Environ. Pathol. Toxicol. Oncol.* **25**(1–2), 29–50 (2006).
9. R. Schmidt, "Photosensitized generation of singlet oxygen," *Photochem. Photobiol.* **82**(5), 1161–1177 (2006).
10. M. J. Niedre et al., "Singlet oxygen luminescence as an *in vivo* photodynamic therapy dose metric: validation in normal mouse skin with topical aminolevulinic acid," *Br. J. Cancer* **92**(2), 298–304 (2005).
11. B. Kruijt et al., "Monitoring ALA-induced PpIX photodynamic therapy in the rat esophagus using fluorescence and reflectance spectroscopy," *Photochem. Photobiol.* **84**(6), 1515–1527 (2008).
12. C. Sheng et al., "Photobleaching-based dosimetry predicts deposited dose in ALA-PpIX PDT of rodent esophagus," *Photochem. Photobiol.* **83**(3), 738–748 (2007).
13. Z. Huang, "A review of progress in clinical photodynamic therapy," *Technol. Cancer Res. Treat.* **4**(3), 283–293 (2005).
14. B. C. Wilson, M. S. Patterson, and L. Lilge, "Implicit and explicit dosimetry in photodynamic therapy: a new paradigm," *Lasers Med. Sci.* **12**(3), 182–199 (1997).
15. P. Nowak-Sliwinska et al., "Study of the pO_2-sensitivity of the dendrimeric and free forms of Pd-meso-tetra(4-carboxyphenyl)porphyrin, incorporated or not in chitosan-based nanoparticles," *Chimia* **65**(9), 691–695 (2011).
16. K. K. Wang et al., "Simulations of measured photobleaching kinetics in human basal cell carcinomas suggest blood flow reductions during ALA-PDT," *Lasers Surg. Med.* **41**(9), 686–696 (2009).
17. M. Forrer et al., "In-vivo measurement of fluorescence bleaching of meso-tetra hydroxy phenyl chlorin (mthpc) in the oesophagus and the oral cavity," *Proc. SPIE* **2627**(1), 33–39 (1995).
18. R. Hornung et al., "Systemic application of photosensitizers in the chick chorioallantoic membrane (CAM) model: photodynamic response of CAM vessels and 5-aminolevulinic acid uptake kinetics by transplantable tumors," *J. Photochem. Photobiol. B* **49**(1), 41–49 (1999).
19. P. Nowak-Sliwinska et al., "Vascular regrowth following photodynamic therapy in the chicken embryo chorioallantoic membrane," *Angiogenesis* **13**(4), 281–292 (2010).
20. N. Lange et al., "A new drug-screening procedure for photosensitizing agents used in photodynamic therapy for CNV," *Invest. Ophthalmol. Vis. Sci.* **42**(1), 38–46 (2001).
21. E. G. Mik et al., "Mitochondrial pO_2 measured by delayed fluorescence of endogenous protoporphyrin IX," *Nat. Meth.* **3**(11), 939–945 (2006).
22. F. Piffaretti et al., "Optical fiber-based setup for *in vivo* measurement of the delayed fluorescence lifetime of oxygen sensors," *J. Biomed. Opt.* **16**(3), 037005 (2011).
23. R. W. Redmond and J. N. Gamlin, "A compilation of singlet oxygen yields from biologically relevant molecules," *Photochem. Photobiol.* **70**(4), 391–475 (1999).
24. M. J. Niedre et al., "Imaging of photodynamically generated singlet oxygen luminescence *in vivo*," *Photochem. Photobiol.* **81**(4), 941–943 (2005).
25. T. K. Stepinac et al., "Light-induced retinal vascular damage by Pd-porphyrin luminescent oxygen probes," *Invest. Ophth. Vis. Sci.* **46**(3), 956–966 (2005).
26. T. Glanzmann et al., "Time-resolved spectrofluorometer for clinical tissue characterization during endoscopy," *Rev. Sci. Instr.* **70**(10), 4067–4077 (1999).
27. E. G. Mik et al., "Mitochondrial pO_2 measured by delayed fluorescence of endogenous protoporphyrin IX," *Nat. Meth.* **3**(11), 939–945 (2006).
28. F. Piffaretti et al., "Optical fiber-based setup for *in vivo* measurement of the delayed fluorescence lifetime of oxygen sensors," *J. Biomed. Opt.* **16**(3), 037005 (2011).
29. D. W. Marquardt, "An algorithm for least-squares estimation of nonlinear parameters," *J. Soc. Indus. Appl. Math.* **11**(2), 431–441 (1963).
30. J. More, "The Levenberg-Marquardt algorithm: implementation and theory," *Numerl. Anal.* **630**(105–116), (1978).
31. E. G. Mik et al., "Excitation pulse deconvolution in luminescence lifetime analysis for oxygen measurements *in vivo*," *Photochem. Photobiol.* **76**(1), 12–21 (2002).
32. G. E. P. Box, G. M. Jenkins, and G. C. Reinsel, "Time series analysis," in *Forecasting and Control*, N. J. W. Hoboken, Ed., pp. 746–755 (2008).
33. A. Fasso, "Residual autocorrelation distribution in the validation data set," *J. Time Ser. Anal.* **21**(2), 143–153 (2000).
34. C. Hoppenheit et al., "Pharmacokinetics of the photosensitizers aminolevulinic acid and aminolevulinic acid hexylester in oro-facial tumors embedded in the chorioallantois membrane of a hen's egg," *Cancer Biother. Radiopharm.* **21**(6), 569–578 (2006).
35. R. Hornung et al., "Systemic application of photosensitizers in the chick chorioallantoic membrane (CAM) model: photodynamic response of CAM vessels and 5-aminolevulinic acid uptake kinetics by transplantable tumors," *J. Photochem. Photobiol. B* **49**(1), 41–49 (1999).
36. M. J. Hammer-Wilson et al., "Photodynamic parameters in the chick chorioallantoic membrane (CAM) bioassay for photosensitizers administered intraperitoneally (IP) into the chick embryo," *Photochem. Photobiol. Sci.* **1**(9), 721–728 (2002).
37. N. Lange et al., "A new drug-screening procedure for photosensitizing agents used in photodynamic therapy for CNV," *Invest. Ophthalmol. Vis. Sci.* **42**(1), 38–46 (2001).
38. S. H. Lim et al., "The neovessel occlusion efficacy of 15-hydroxy-purpurin-7-lactone dimethyl ester induced with photodynamic therapy," *Photochem. Photobiol.* **86**(2), 397–402 (2010).
39. S. Lee et al., "Pulsed diode laser-based singlet oxygen monitor for photodynamic therapy: *In vivo* studies of tumor-laden rats," *J. Biomed. Opt.* **13**(6), 064035 (2008).
40. B. C. Wilson and M. S. Patterson, "The physics, biophysics, and technology of photodynamic therapy," *Phys Med Biol* **53**(9), R61–109 (2008).
41. M. T. Jarvi et al., "Singlet oxygen luminescence dosimetry (SOLD) for photodynamic therapy: current status, challenges and future prospects," *Photochem. Photobiol.* **82**(5), 1198–1210 (2006).

42. I. Georgakoudi and T. H. Foster, "Singlet oxygen- versus nonsinglet oxygen-mediated mechanisms of sensitizer photobleaching and their effects on photodynamic dosimetry," *Photochem. Photobiol.* **67**(6), 612–625, (1998).
43. A. P. Castano, T. N. Demidova, and M. R. Hamblin, "Mechanisms in photodynamic therapy: Part 1—Photosensitizers, photochemistry, and cellular localization," *Photodiag. Photodyn. Ther.* **1**(4), 279–293 (2004)
44. E. G. Mik et al., "*In vivo* mitochondrial oxygen tension measured by a delayed fluorescence lifetime technique," *Biophys J.* **95**(8), 3977–3990 (2008).
45. J. Grote, R. Susskind, and P. Vaupel, "Oxygen diffusivity in tumor tissue (DS-carcinosarcoma) under temperature conditions within the range of 20–40°C," *Pflugers Arch.* **372**(1), 37–42 (1977).
46. J. Moan and K. Berg, "The photodegradation of porphyrins in cells can be used to estimate the lifetime of singlet oxygen," *Photochem. Photobiol.* **53**(4), 549–553 (1991).
47. K. Plaetzer et al., "Photophysics and photochemistry of photodynamic therapy: fundamental aspects," *Lasers Med. Sci.* **24**(2), 259–268 (2009).
48. M. Ascencio et al., "Comparison of continuous and fractionated illumination during hexaminolaevulinate-photodynamic therapy," *Photodiag. Photodyn. Ther.* **5**(3), 210–216 (2008).
49. K. K. Wang et al., "Irradiation-induced enhancement of Pc 4 fluorescence and changes in light scattering are potential dosimeters for Pc 4-PDT," *Photochem. Photobiol.* **83**(5), 1056–1062 (2007).
50. P. Uehlinger et al., "On the role of iron and one of its chelating agents in the production of protoporphyrin IX generated by 5-aminolevulinic acid and its hexyl ester derivative tested on an epidermal equivalent of human skin," *Photochem. Photobiol.* **82**(4), 1069–1076 (2006).
51. P. Nowak-Sliwinska et al., "Processing of fluorescence angiograms for the quantification of vascular effects induced by anti-angiogenic agents in the CAM model," *Microvasc. Res.* **79**(1), 21–28 (2010).
52. E. Debefve et al., "Video monitoring of neovessel occlusion induced by photodynamic therapy with verteporfin (Visudyne), in the CAM model," *Angiogenesis* **11**(3), 235–243 (2008).
53. T. H. Foster et al., "Oxygen consumption and diffusion effects in photodynamic therapy," *Radiat. Res.* **126**(3), 296–303 (1991).
54. A. T. Nathan and M. Singer, "The oxygen trail: tissue oxygenation," *Br. Med. Bull.* **55**(1), 96–108 (1999).
55. T. Schunck and P. Poulet, "Oxygen consumption through metabolism and photodynamic reactions in cells cultured on microbeads," *Phys. Med. Biol.* **45**(1), 103–119 (2000).
56. K. Plaetzer et al., "Photophysics and photochemistry of photodynamic therapy: fundamental aspects," *Lasers Med. Sci.* **24**(2), 259–268 (2009).
57. A. F. Cruess et al., "Photodynamic therapy with verteporfin in age-related macular degeneration: a systematic review of efficacy, safety, treatment modifications, and pharmacoeconomic properties," *Acta. Ophthalmol.* **87**(2), 118–132 (2009).